Pol. J. Environ. Stud. Vol. 31, No. 3 (2022), 2255-2263
DOI: *10.15244/pjoes/144551*

Original Research

Traceability of Nitrogen and Oxygen Isotopes in Nitrates with the SIAR Model: Case Study on the Wangbeng Interval of the Huaihe River Basin

Rongrong Tong[1], Liangmin Gao[1]*, Zhendong Pang[2], Xin Gu [3], Xiaoqing Chen[1], Jinxin Zhang[1], Hui Wang[1], Shuo Wang[1], Chuang Shi[1], Xudong Chen[1]

[1]School of Earth and Environment, Anhui University of Science and Technology, Huainan, China
[2]Environmental Protection Monitoring Station of Huainan city, Huainan, China
[3]Jiangsu Geological Prospecting Team Three, Changzhou, Jiangsu, China

Received: 24 September 2021
Accepted: 5 December 2021

Abstract

The identification of non-point nitrate sources is important for the study and management of non-point pollution sources in agricultural areas. In this study, the nitrogen and oxygen dual-isotope technique and the Stable Isotope Analysis in R (SIAR) model were used to qualitatively and quantitatively analyze nitrate sources in the Huaihe River basin in China. The results showed that the inorganic nitrogen in the water was mainly in the form of nitrate nitrogen with a mean concentration of 1.32 mg/L. In the middle section, the major pollution sources were manure and domestic sewage (43.46%) and soil (30.23%), followed by chemical fertilizer (14.56%), dead branches and fallen leaves (8.18%), and atmospheric deposition (3.55%). Chemical fertilizers due to farmland cultivation were a bigger pollution source in the upper reaches (28.73%) than in the middle reaches (5.76%) and downstream (4.37%). Chemical fertilizers (74.86%) were the main pollution source on the south bank, while soil (34.43%), manure and domestic sewage (33.24%), and chemical fertilizers (29.31%) were the main pollution sources on the north bank. The main sources of NO3- were soil, chemical fertilizer, excrement and domestic sewage. Atmospheric deposition and dead leaves were the secondary sources of nitrate pollution. Major pollution sources comprised a large proportion of the total pollution (89.67%) compared to secondary pollution sources (10.33%). These findings highlight the significant impacts of manure, domestic sewage, and agricultural fertilizer, and they can be used to support nitrogen management practices in agricultural areas.

Keywords: water pollution, SIAR model, source resolution, isotope

---

*e-mail: gaolmin@163.com

Introduction

Water bodies subjected to intensive human activities have seen increased nitrogen content in recent decades, which has led to severe degradation of the aquatic environment [1, 2]. This has become a potential risk to human survival and health, and it is an important obstacle to the sustainable development of the economy and society [3]. Nitrate is the main form of nitrogen in surface rivers, and a greater nitrate concentration than is suitable for the ecosystem can cause significant harm to humans and the ecological environment [3-5]. Most nitrate pollution of surface water is due to human activities, such as agriculture, urban waste, and industry [6, 7]. Excessive and improper use of chemical fertilizers in agriculture increases the nitrate content in the soil, which transfers to the watershed through runoff and leaching processes and affects the aquatic environment. Manure and domestic sewage are the other major agricultural sources of nitrate in river basins [8].

Understanding the source of nitrate in the river basin is necessary for eliminating nitrogen pollution from the water [9]. Traditional approaches to identifying nitrate sources combine the land use type with hydrogeochemical theory, but the results have significant uncertainty because of the complexity of the nitrate migration and transformation processes and the dispersion and concealment of pollution sources [10]. Advances in isotope identification technology and the fact that different nitrate sources have different stable isotope characteristics have led to the wide application of the nitrogen and oxygen dual-isotope technique for determining nitrate sources in water [11]. Nitrate nitrogen and oxygen isotopes can be coupled with Bayesian mixing models to provide a powerful tool for quantitatively identifying the mixing ratios of different nitrate sources [12].

The Huaihe River basin is the main producer of China's grain. The agricultural non-point source pollution in this basin is mainly fertilizers and pesticides from farmland and untreated domestic sewage from rural life. Precipitation causes pollutants to enter the groundwater and surface water through surface runoff and underground storage and infiltration, which pollutes the receiving water body. In this study, quantitative and qualitative analyses were performed on the nitrogen pollution of the Huaihe River basin and the main pollution sources. The study comprised three main components: characterizing the water quality, qualitatively analyzing the nitrate sources, and quantifying the contributions of nitrate sources within the study area and the effects of human activities and farming practices [13]. This study should help demonstrate the applicability of isotope technology to pollution prevention and control of water environments and provide a scientific basis for river basin management.

Experimental

Overview of the Study Area

The study area mainly comprised the middle section of the Wangbeng interval in the Huaihe River basin, which includes Chengdong Lake on the south bank and Nihe River on the north bank. The sampling points were located within longitudes of 111°55′-121°20′E and latitudes of 30°55′-6°20′N. The basin has a warm temperate climate north of the Huaihe River and a subtropical climate south of it. The annual average temperature and average precipitation in the basin are 11-16ºC and 900 mm, respectively [14]. Mountainous and coastal areas have more rainfall compared to the plains and inland at the same latitude. The rainfall has a large inter-annual variation with uneven spatial and temporal distributions, which makes utilizing the water resources difficult [15]. The area of cultivated land in the Huaihe River Basin is 133,300 km^2. The main crops are wheat, rice, corn, potato, soybean, cotton and rape. The total population is 165 million Chengdong Lake is east of Huoqiu County, Lu'an City, Anhui Province, China. It has a subtropical humid monsoon climate with four distinct seasons, abundant sunlight, and abundant rainfall. The lake is long and narrow, with a width of 5.0 km from east to west and a length of 39.0 km from north to south. It has a total drainage area of 110 km and is located at the lower reaches of the Jihe River, which is a tributary of the Huaihe River. It is an important flood storage area for the middle reaches of the Huaihe River, a national-level ecological reserve, and an important source of drinking water [16]. The Nihe River is a tributary of the north bank of the Huaihe River, and it is located in Huainan City and Huaiyuan County in north-central Anhui Province, China. The Nihe River originates from the hydroelectric power plant of Tanglugou on the south bank of the Cihuai New River and flows east to south into Panji District of Huainan City, where it converges with the Heihe River southeast of the Panji District. Here, the river widens from 300 m to 1100 m. After the confluence, the Nihe River flows into the Huaihe River through the Qingnian Sluice and Tangyu Lake flood discharge area to the Yinjiagou Sluice. The river has a total length of 62 km and a drainage area of 606 km^2 [17].

Sample Collection and Measurement

The study area was centered on the middle section of the Huaihe River (14 samples), Chengdong Lake to represent the north bank (four samples), and the Nihe River to represent the south bank (four samples). Samples were taken from November 2020 to January 2021, and the sampling points are shown in Fig. 1. For each sample, 2 L of water was taken and refrigerated in a high-density polyethylene bottle. Part of each sample was acidified with sulfuric acid until the pH was

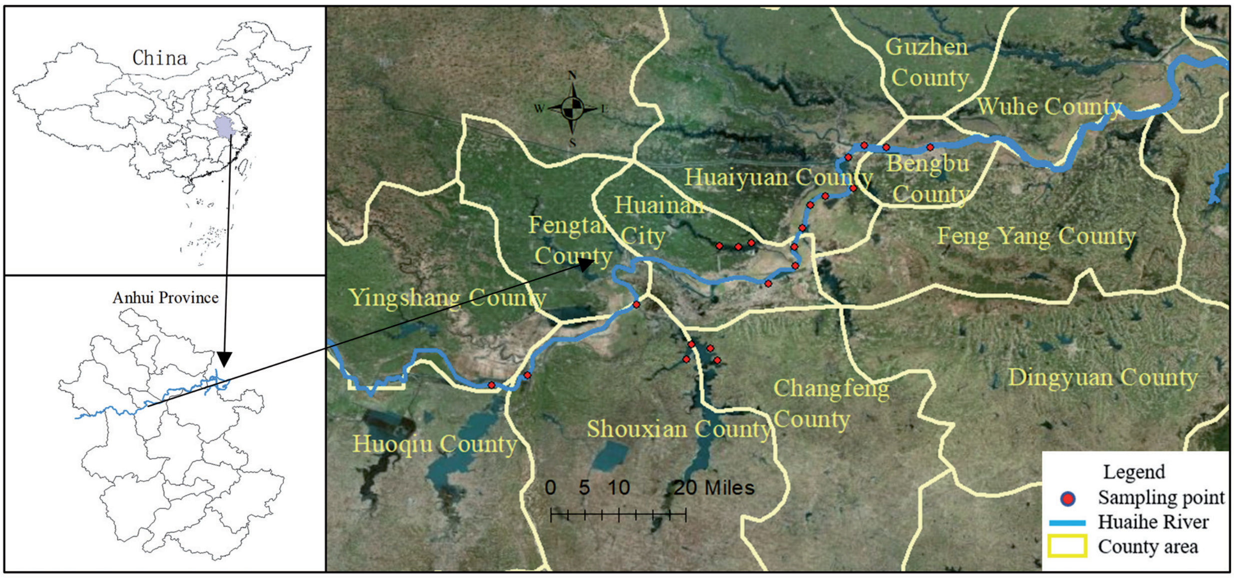

Fig. 1. Sampling map of the study area.

less than 2. The pH, dissolved oxygen (DO), turbidity, total dissolved solids (TDS), and water temperature of the samples were measured onsite by using a portable water quality detector. The samples were divided into two groups. Group A comprised 22 samples, which were analyzed for water quality with the alkaline potassium persulfate digestion UV spectrophotometry method (HJ 636-2012). Then, the total nitrogen (TN), total phosphorus (TP), ammonia nitrogen (NH_3^-–N), nitrate nitrogen (NO_3^-–N), and chemical oxygen demand (COD_{Mn}) were determined by using the ammonium molybdate spectrophotometry method (GB 11893-89), Nessler's reagent spectrophotometry (HJ 535-2009), ultraviolet spectrophotometry (HJ/T 346-2007), and dichromate method (HJ 828-2017), respectively [18]. The 14 samples in Group B were tested for nitrate nitrogen and oxygen isotopes (i.e., $\delta^{15}N–NO_3^-$ and $\delta^{18}O–NO_3^-$) on a full analytical basis. Then, the denitrification bacteria method was used to determine the stable $\delta^{15}N–NO_3^-$ and $\delta^{18}O–NO_3^-$ isotopes. This method is based on adding denitrification bacteria that cannot catalytically reduce nitrous oxide (N_2O) to nitrogen (N_2) (i.e., *Pseudomonas aureofaciens*) to convert all NO_3^-–N in the sample to N_2O. The generated N_2O is separated and purified; it is then placed within the isotope ratio mass spectrometer to determine $\delta^{15}N–NO_3^-$ and $\delta^{18}O–NO_3^-$. The determined $\delta^{15}N–NO_3^-$ and $\delta^{18}O–NO_3^-$ values can be compared with standard samples of the atmosphere (air) and Vienna Standard Mean Ocean Water (V-SMOW), respectively, to determine the source of NO_3^- pollution in water bodies [19]:

$$\delta R_{sample}(‰) = \left(\frac{R_{sample}}{R_{standard}} - 1\right) \times 1000 \tag{1}$$

where δR_{sample} is the relative deviation in heavy and light isotopes between the test and standard samples (thousandths), R_{sample} is the ratio between the heavy and light isotopes of the test sample, and $R_{standard}$ is the ratio between the heavy and light isotopes of the standard sample.

In addition, potential sources of NO_3^- pollution in the study area were collected to analyze the characteristic values of $\delta^{15}N–NO_3^-$ and $\delta^{18}O–NO_3^-$. These sources included soils of different land use types (nine), sewage (nine including domestic sewage and livestock and poultry manure), and litter (four). The land use types of soil as pollution sources in this research area mainly include farmland, forest land and grassland. The pollution of farmland mainly comes from planting and fertilization, while the forest land and grassland are mainly from livestock and poultry excrement. The solid sample isotope test method was used for detection.

Isotope Source Analysis Model (SIAR)

The Stable Isotope Analysis in R (SIAR) model is based on the R statistical software developed by Parnell [20]. The Dirichlet distribution is used to represent the prior distribution of contributions by each pollutant. Then, the Bayesian method is used to analyze the posterior distribution of the contributions after the observation data are obtained. When defined with N measurements, J isotopes, and K sources, the SIAR model can be expressed as follows:

$$X_{ij} = \frac{\sum_{k-1}^{k} p_k q_{jk}(s_{jk} + c_{jk})}{\sum_{k-1}^{k} p_k q_{jk}} + \varepsilon_{ij} \tag{2}$$

$$S_{jk} \sim N\left(\mu_{jk}, \omega_{jk}^2\right) \tag{3}$$

$$c_{jk} \sim N\left(\lambda_{ij}, \tau_{jk}^2\right) \tag{4}$$

$$\varepsilon_{ij} \sim N\left(0, \sigma_j^2\right) \tag{5}$$

where X_{ij} is the δ value of isotope j of mixture I and P_k is the proportion of source k to be calculated. S_{jk} is the δ value of source k and isotope j, and it obeys a normal distribution with a mean μ and variance ∞. c_{jk} is the fractionation coefficient of source k and isotope j, and it obeys a normal distribution with a mean λ and variance τ. ε_{ij} is the residual error of the ratio of isotope j in the mixed sample i, and it represents the unquantifiable variance among other mixtures.

The SIAR model was used to calculate the various sources of NO_3^- pollution in the water body and the variation in different seasons [21]. The SIAR model has been shown to account for the spatial differences of isotopes in the pollution source and receiving water body to minimize the uncertainty in the calculation results [22]. Moreover, it is applicable to multiple pollution sources and is not limited by the number of isotopes. Compared with other identification methods, it is more flexible to be applied. Thus, it was considered suitable for this study area., but this model requires high R language software application ability, which is higher than the traditional method.

Results and Discussion

Water Quality Characterization

The water quality is characterized by the TN, which includes inorganic nitrogen such as NO_3^-–N, NH_4^+–N, and nitrite nitrogen (NO_2^-–N) and organic nitrogen such as protein, amino acids, and organic amines. TN, NO_3^-–N, and NH_4^+–N are often used to characterize the severity of water pollution [23]. Table 1 indicates that the water in the study area was slightly alkaline. The TN concentration was 1.26-8.07 mg/L with an average of 3.34 mg/L, the NO_3^-–N concentration was 0.11-2.39 mg/L with an average of 1.32 mg/L, and the NH_4^+–N concentration was 0.30–5.59 mg/L with an average of 0.90 mg/L. The dominant form of nitrogen was NO_3^-–N, which accounted for about 40% of the TN. The DO concentration had a wide range of 2.28-6.69 mg/L with an average of 5.51 mg/L, which indicates that the DO concentration was high at most sampling points. Nitrification is not limited when DO >5 mg/L, so NH_4^+–N in the water body was smoothly converted into NO_3^-–N. The average TP concentration indicated that the water met the Class II standard, and the average COD indicated that the water met the Class III standard.

Qualitative Analysis of the Source of Nitrate in the Study Area

The characteristic values of $\delta^{15}N–NO_3^-$ and $\delta^{18}O–NO_3^-$ needed to be determined for the qualitative and quantitative analyses on the NO_3^- sources in the study area [24]. The pollution sources of the study area were divided into five major categories: manure and domestic sewage (MS), soil sources (SN), atmospheric deposition (AP), chemical fertilizers (FS), and dead branches and fallen leaves (DF). The $\delta^{15}N–NO_3^-$ and $\delta^{18}O–NO_3^-$ values for MS, SN, and DF were obtained in this study, while the $\delta^{15}N–NO_3^-$ and $\delta^{18}O–NO_3^-$ for other pollution sources were taken from the literature [25], as given in Table 2.

Because different sources of NO_3^-–N pollution have different $\delta^{15}N$ and $\delta^{18}O$ values, the isotopic composition can be used to qualitatively identify NO_3^-–N sources [26]. However, the multiple nitrogen cycles of agricultural activities cause isotope fractionation [27]. Among these nitrogen cycles, denitrification has the greatest impact by changing the composition of NO_3^- isotopes and affecting their traceability. Understanding the presence of denitrification is a prerequisite for exploring NO_3^- sources [11]. Previous studies have shown that a ratio of $\delta^{15}N$ to $\delta^{18}O$ between 1.3:1 and 2.1:1 is a good indicator of denitrification [28,29]. In the denitrification process, microorganisms transform NO_3^- into N_2O and N_2, and light isotopes are preferentially used in these processes due to isotope fractionation. Therefore, when denitrification occurs, The $\delta^{15}N$-NO_3^- and $\delta^{18}O$- NO_3^- values increase with the decrease of ρ (NO_3^-). When the increment ratio of $\delta^{18}O$-NO_3^- and $\delta^{18}O$-NO_3^- of NO_3^- is in the range of 1.3 ~ 2.1, it indicates that denitrification has taken place. Most of the samples were outside the range of the denitrification ratio (Fig. 2). In addition, denitrification usually increases $\delta^{15}N–NO_3^-$ and decreases the NO_3^-–N concentration. Thus, the relationship between $\delta^{15}N–NO_3^-$ and the NO_3^-–N concentration can be used to reveal the reaction processes occurring in the water column. Fig. 3 shows that the NO_3^-–N concentration had an obvious positive

Table 1. Basic water quality data.

	pH	TDS (mg·L^{-1})	COD (mg·L^{-1})	NO_3^--N (mg·L^{-1})	NH_4^+-N (mg·L^{-1})	TN (mg·L^{-1})	TP (mg·L^{-1})	DO (mg·L^{-1})
Average value	8.05	0.32	21.50	1.32	0.90	3.34	0.30	5.51
Minimum value	7.54	0.10	7.01	0.11	0.30	1.26	0.10	2.28
Maximum value	8.56	0.49	42.16	2.39	5.95	8.07	0.72	6.69
Standard deviation	0.25	0.10	9.06	0.77	1.17	1.50	0.17	1.21

Table 2. Nitrogen and oxygen isotope signature values for different sources of nitrate pollution.

Source of pollution	$\delta^{15}N$		$\delta^{18}O$		Source
	Average value	Standard deviation	Average value	Standard deviation	
Atmospheric deposition (AP)	-1.49	1.75	58.18	14.22	Literature [25]
Soil sources (SN)	7.46	2.11	4.23	1.08	Self-test
Chemical fertilizers (FS)	-0.53	0.22	2.96	1.69	Literature [25]
Manure and domestic sewage (MS)	8.92	1.57	4.36	0.91	Self-test
Dead branches and fallen leaves (DF)	-0.05	0.95	22.08	2.36	Self-test

correlation with $\delta^{15}N–NO_3^-$ with a correlation coefficient of 0.67. These results indicate that most of the water bodies in the study area did not undergo denitrification [30].

As shown in Fig. 2, the $\delta^{15}N–NO_3^-$ and $\delta^{18}O–NO_3^-$ values of samples were characteristic of three NO_3^--N sources: MS, SN, and FS. This indicates that they were the main sources of NO_3^- pollution in the water column of the study area. The $\delta^{15}N–NO_3^-$ and $\delta^{18}O–NO_3^-$ values were –5.14‰-17.18‰ and 5.11‰-13.38‰, respectively, for the middle section; −13.71‰-7.34‰ and 4.70‰-13.38‰, respectively, for the south bank; and 0.94‰-17.10‰ and 1.85‰-12.36‰, respectively, for the north bank. Compared to MS and SN, which are sources of organic nitrogen, AP and DF are characterized by lower $\delta^{15}N–NO_3^-$ and higher $\delta^{18}O–NO_3^-$. Thus, Fig. 2 indicates that AP and DF made small contributions to the NO_3^- concentration in the study area.

Meanwhile, agricultural activities were intensive, and FS made a significant contribution to the NO_3^- concentration. The main sources of NO_3^- in the water bodies of the study area were concluded to be SN, FS, and MS. AP and DF were secondary sources of NO_3^- pollution. The $\delta^{15}N–NO_3^-$ values of the middle section of the Huaihe River covered a wide range and should be further divided to study the effect of individual pollution sources. The specific contribution of each source could not be obtained from the analysis of the $\delta^{15}N–NO_3^-$ and $\delta^{18}O–NO_3^-$ values. Therefore, the SIAR model was used to quantitatively resolve the NO_3^- sources [30].

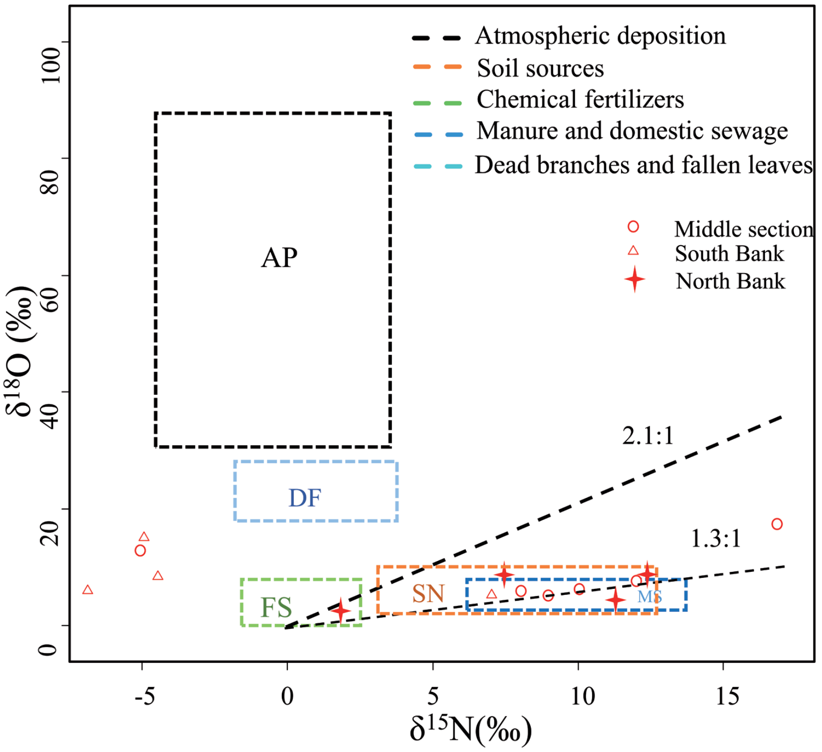

Fig. 2. Nitrogen and oxygen isotopic ranges of typical nitrate end components and the distribution of nitrate nitrogen and oxygen relationships in the water column of the study area.

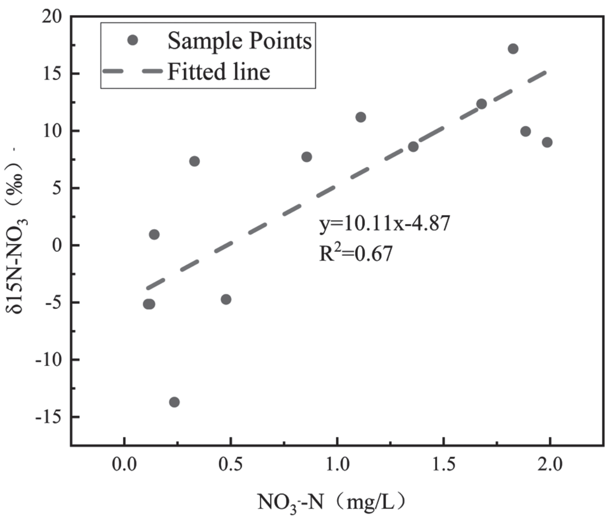

Fig. 3. Plot of $\delta^{15}N–NO_3^-$ versus $NO_3^-–N$ concentrations.

Quantitative Analysis of Nitrate Sources in the Study Area

Nitrate Sources in the Middle Section of the Wangbeng Interval in the Huaihe River Basin

The water bodies of the Wangbeng interval of the Huaihe River basin are mainly affected by nitrification with little denitrification. Assuming no isotopic fractionation and a nitrogen isotopic enrichment coefficient of nitrification ε = 0‰ [7], the contributions of the five types of pollution sources can be calculated by using the SIAR model. Fig. 4 shows that the contributions of the five types of pollution sources differed among the upper, middle, and lower reaches of the Huaihe River. In the upper reaches, NO_3^- mainly came from SN (25.49%), FS (28.73%), and MS (24.98%). In the middle reaches, NO_3^- mainly came from SN (29.77%) and MS (51.25%). In the lower reaches, NO_3^- mainly came from SN (35.47%) and MS (54.16%). Overall, the largest NO_3^- contribution came from MS (43.46%), followed by SN (30.23%), FS (14.56%), MS (8.18%), and AP (3.55%).

Differences in Nitrate Sources between the Middle of the Huaihe River and on the North and South Banks

The SIAR model was used to calculate the contributions of the five pollution sources to the middle section and the north and south banks of the Huaihe River Basin. The results are shown in Fig. 5. For the middle section, the main pollution sources were SN (36.54%) and MS (45.96%). For the south bank, the main pollution source was FS (74.86%), which may have been exacerbated by agricultural activities and runoff from the surrounding farmland. For the north bank, main pollution sources were SN (34.43%), MS (33.24%), and FS (29.31%). Overall, the biggest pollution source for all three sections was FS (37.06%), followed by MS (28.13%), SN (25.67%), DF (6.43%), and AP (2.71%).

These results indicate that the main NO_3^- sources for the middle section were SN, FS, and MS, which are representative of agricultural non-point source pollution. This indicates that the study area is severely polluted by agricultural activities, and AP and DF are secondary sources of NO_3^- pollution. The results of the quantitative analysis with the SIAR model are consistent with the results of the qualitative analysis. Fig. 6 compares the total contributions of major sources (SN + FS + MS) and minor sources (AP + DF) in the study area for different parts. On average, the major sources contributed 89.67%, which is much greater than the contribution of minor sources (10.33%). The total contribution of major sources increased from upstream to downstream in the middle section. Major sources made up 99% of the total contribution downstream, which indicates that agricultural pollution and human activities had a far greater effect than rainfall and plant residue. The total contribution of major pollution sources was lowest for the south bank and highest for

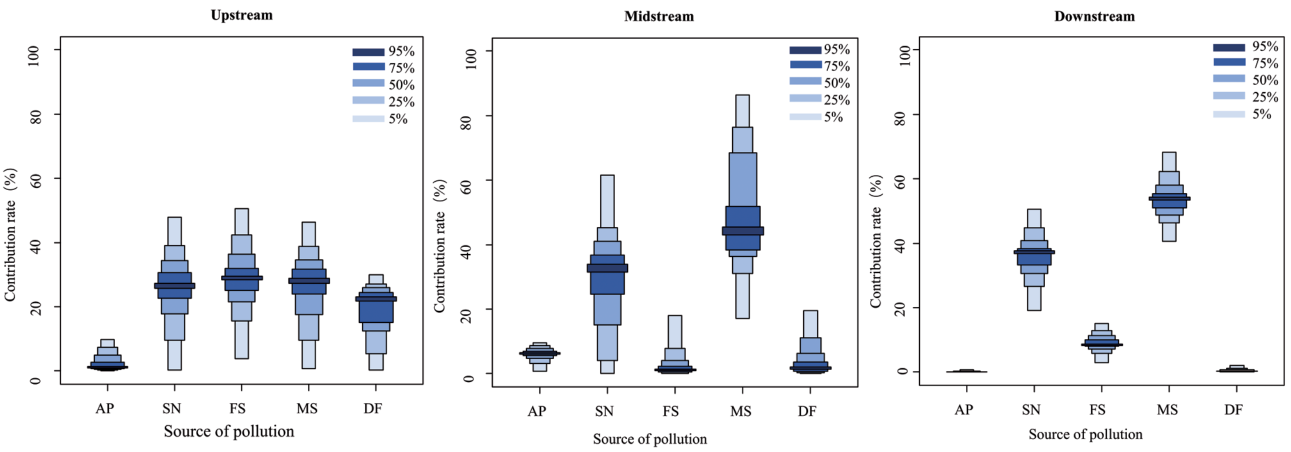

Fig. 4. Calculated contributions of the five types of pollution sources to the middle section of the Wangbeng interval in the Huaihe River basin according to the SIAR model (Box plot legend: 5%, 25%, 50%, 75%, and 95% scales from light to dark).

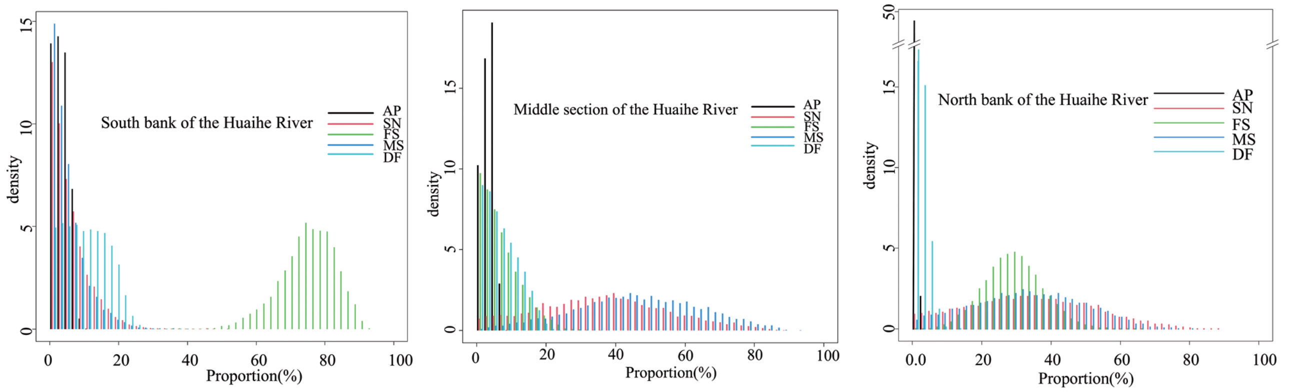

Fig. 5. Distributions of the five types of pollution sources in the middle section and on the north and south banks of the Huaihe River./

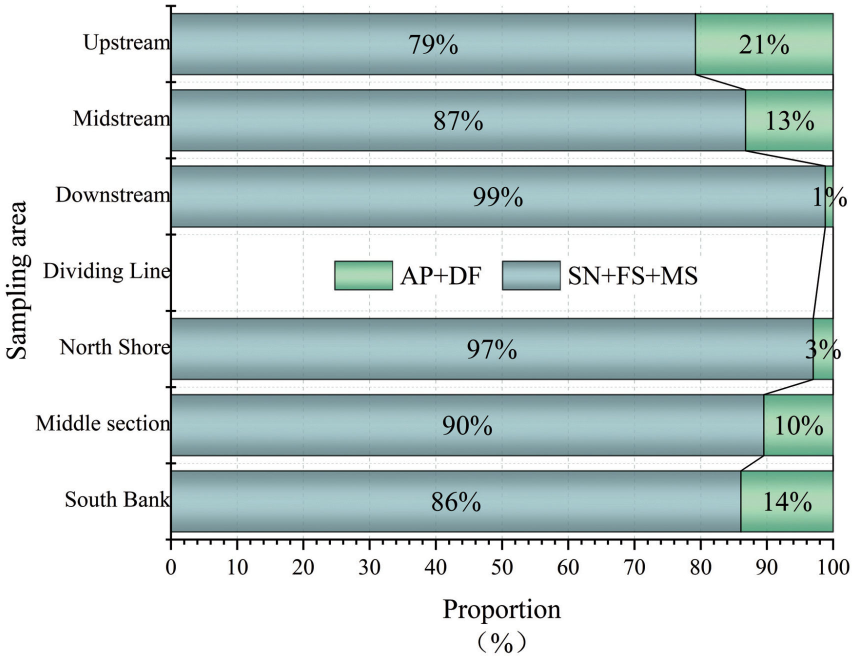

Fig. 6. Comparison of the shares of major and minor pollution sources.

the north bank. Major pollution sources made up 97% of the pollution for the north bank. The sampling points for the south bank were close to the upper reaches of the middle section, and the sampling points for the north bank were close to the lower reaches. Thus, the downstream area was close to towns and was greatly affected by urbanization and farmland. In summary, the traceability of pollutant isotopes shows that the middle section of the Wangbeng interval of the Huaihe River basin is heavily polluted by urbanization and farmland owing to its proximity to towns. The main pollution sources are MS and FS, which should be controlled.

Conclusions

The water bodies in the middle section of the Wangbeng interval and the north and south banks of the Huaihe River basin are mainly polluted by nitrogen in the form of NO_3^-–N. The middle section is the most polluted, and human activities and farmland cultivation are clearly the most significant influences. The SIAR model results indicated that NO_3^-–N in the middle section of the Huaihe River mainly comes from MS (43.46%), SN (30.23%), and FS (14.56%). FS had a greater influence on water bodies in the upper reaches than in the middle and lower reaches because the upper reaches are surrounded by farmland. The main pollution sources are FS (74.86%) for the south bank and SN (34.43%), MS (33.24%), and FS (29.31%) for the north bank. The south bank is more obviously affected by agriculture. The total contribution of major pollution sources was much greater than that of secondary pollution sources. Thus, agricultural non-point sources are the main contributor to nitrogen pollution in water bodies in the study area.

In this study, the SIAR model was used to study qualitatively and quantitatively the contribution rate of nitrate sources in the middle section of the Wangbeng interval and the north and south banks of the Huaihe River basin. However, some limitations need to be considered. During the migration and transformation of water nitrogen, the nitrification and denitrification can cause the fractionation of nitrogen, which may, in turn, affect the contents of δ^{15}Nand δ^{18}O. In this study, C_{jk} was defined as 0 and the fractionation was neglected, which may lead to the deviations of the calculation. In future studies, the effect of the isotope fractionation should be incorporated in the SIARmodel to more accurately track and quantify the nitrogen pollutants.

Acknowledgments

We sincerely thank the editors and reviewers for their valuable time to review the paper. This work was supported by the Ecological Environment Special Project of Key Research and Development Program of Anhui Province(202004i07020012).

Conflict of Interest

The authors declare no conflict of interest.

References

1. KOU X.Y., DING J.J., LI Y.Z., LI Q.Z., MAO L.L. Tracing nitrate sources in the roundwater of an intensive agricultural region. Agricultural Water Management. **250** (8), 106826 **2021**.
2. BIDDAU R., CIDU R., PELO DA., CARLETTI A., GHIGLIERI G., PITTALIS D. Source and fate of nitrate in contaminated groundwater systems: assessing spatial and temporal variations by hydrogeochemistry and multiple stable isotope tools. Science of The Total Environment, **647** (PT.1-1664), 1121, **2018**.
3. XUE D.M., BOTTE J., DE B.D., ACCOE F., NESTLER A., TAYLOR P., VAN T.O., BERGLUND M., BOECKX P. Present limitations and future prospects of stable isotope methods for nitrate source identification in surface and groundwater. Water research, **43** (5), 1150, **2008**.
4. XUE D.M., DE B.B., VAN C.O., HENNESSY C., BERGLUND M., BOECKX P. Use of a Bayesian isotope mixing model to estimate proportional contributions of multiple nitrate sources in surface water. Environmental pollution (Barking, Essex: 1987), **161**, 43, **2012**.
5. YANG L.P., HAN J.P., XUE J.L., ZENG L.Z., SHI J.C. Nitrate source apportionment in a subtropical watershed using bayesian model. Science of The Total Environment, **463-464** C (5), 340, **2013**.
6. MA G.W., WANG Y.Y., BAO X., HU Y., LIU Y.P., HE L.H., WANG T.M., MENG F.S. Nitrogen pollution characteristics and source analysis using the stable isotope tracing method in Ashi River, northeast China. Environmental Earth Sciences, **73** (8), **2015**.
7. JIN Z.F., QIAN L.J., SHI Y.S., FU G.W., LI G.Y., LI F.L. Quantifying major NOx sources of aerosol nitrate in Hangzhou, China, by using stable isotopes and a Bayesian isotope mixing model. Atmospheric Environment, **244**, 117979, **2021**.
8. COURAGE D.E., GEOPHREY K.A., SAMUEL Y.G., EMMANUEL K.A., SI-LIANG L., SAMUEL B.D. Nitrate contamination of groundwater in the Lower Volta River Basin of Ghana: Sources and related human health risks. Ecotoxicology and Environmental Safety, **191**, 5674, **2020**.
9. ZHANG Q.Q., WANG H.W. Assessment of sources and transformation of nitrate in the alluvial-pluvial fan region of north China using a multi-isotope approach. Journal of Environmental Sciences, **89**, 9, **2020**.
10. KORTH F., DEUTSCH B., FREY C., MOROS C., VOSS M. Nitrate source identification in the baltic sea using its isotopic ratios in combination with a bayesian isotope mixing model. Biogeosciences, **11**(17), 4913, **2014**.
11. ZHAO Y., DANG J.H., WANG F., FENG C.L. Sources of Nitrogen Pollution in Upstream of Fenhe River Reservoir Based on the Nitrogen and Oxygen Stable Isotope. Journal of Chemistry, **2020**, 1, **2020**.
12. LI X.X., WU P., ZHA X.F., HE S.Y., WU L.N., HAN Z.W. Tracing nitrate sources in urban waters of Karst mountainous area usinghydrochemistry and stable isotope. Acta Scientiae Circumstantiae, **41** (03), 12, **2020**.
13. LIU X.L., HAN G.L., ZENG J., LIU M., LI X.Q., BOECKX P. Identifying the sources of nitrate contamination using a combined dual isotope, chemical and Bayesian model approach in a tropical agricultural river: Case study in the Mun River, Thailand. The Science of the total environment, **760**, **2020**.
14. GAO C., TIAN R. The influence of climate change and human activities on runoff in the middle reaches of the huaihe river basin, china. Journal of Geographical Sciences, **28** (1), 79-92, **2018**.
15. ZHOU L., XU J.G., JIANG J., YUAN Y.H., SUN D.Q. Spatial diversity characteristics of comprehensive control ability for water environmental pollution in the huaihe river basin. Progress in Geography, **32** (4), 560, **2013**.
16. ZHAO X.X., LU W.X., LI J., LIANG Y.Y., FANG T. Community structure of phytoplankton and bio-assessment of water quality in Chengdong Lake in Anhui, China. Ecological Science, **39** (5), 187, **2020**.
17. LI J. Study on Flood Storage and WaterLogging Control in middle course of Huaihe river Mining Subsidence Area. China Institute of Water Resources & Hydropower Research, Beijing, **2013**.
18. LU Y.G., LIU F., YAO H., YU X.H., ZHANG S.C., CANG X.H. Source analysis of nitrate pollution source in groundwater in A Small Watershed of Miyun Reservoir in Beijing. Environmental Chemistry, **35** (1), 180, **2016**.
19. GAO L.R., XIA D., TIAN H.Z., ZHANG H.J., LIU L.D., WANG Y.W. Concentrations and distributions of 18 organochlorine pesticides listed in the Stockholm Convention in surface sediments from the Liaohe River basin, China. Journal of environmental science and health. Part. B, Pesticides, food contaminants, and agricultural wastes. **50** (5), 322, **2015**.
20. ABASS G., JOSEPH R.F., SAMUEL G., DICKSON A., GEOPHREY A., NAFISATU Z. Nitrate contamination and source apportionment in surface and groundwater in Ghana using dual isotopes (^{15}N-NO$_3$- and ^{18}O-NO$_3$-) and a Bayesian isotope mixing model. Journal of Contaminant Hydrology, **233**, 103658, **2020**.

21. ANDREW C.P., RICHARD I., STUART B., ANDREW L.J. Source Partitioning Using Stable Isotopes: Coping with Too Much Variation. PLOS ONE, **5** (3), 9672, **2010**.
22. KANG P.P., XU S.G. The study on contribution of nitrate source to groundwater in the east coast of Laizhou Bay based on isotopemixing model. Water Resources and Hydropower Engineering, **51** (11), 155, **2020**.
23. JOHNSON S.R., BURCHELL M.R., EVANS R.O., OSMOND D.L., GILLIAM W. Riparian buffer located in an upland landscape position does not enhance nitrate-nitrogen removal. Ecological Engineering, **52**, 252, **2013**.
24. YEON J., GAUTAM M.K., KIM L., LEE S., LEE D. Isotopic composition of throughfall nitrates in suburban forests with different vegetations. Geosciences Journal, **19** (1), 167, **2015**.
25. FAZEKAS H.M., WYMORE A.S., MCDOWELL W.H. Dissolved organic carbon and nitrate concentration-discharge behavior across scales: land use, excursions, and misclassification. Water Resources Research, **56** (8), **2020**.
26. WEI S.C., LIU J.T., XIA J.B., MA L. Analysis of surface water and groundwater nitrate sources in Binzhou City in the Yellow River Delta using isotopes of nitrogen and oxygen. Journal of Beijing Normal University (Natural Science), **57** (01), 29, **2021**.
27. ZHAO Q.L., MA H.Y., REN Y.F., WANG X.K., PENG J.F. $\delta^{15}N\text{-}NO_3$-and $\delta^{18}O\text{-}NO_3$-Tracing of Nitrate Sources in Beijing Urban Rivers. Environmental Sciences, **37** (05), 1692, **2016**.
28. ZHAO H., XU Y., CHENG S.Q., LI Q.L., YU H.R. Application of the dual-isotope approach and Bayesian isotope mixing model to identify nitrate in groundwater of a multiple land-use area in Chengdu Plain, China. Science of the Total Environment, **717** (5), 137134.1-137134.12, **2020**.
29. JI X.L., XIE R.T., HAO Y., LU J. Quantitative identification of nitrate pollution sources and uncertainty analysis based on dual isotope approach in an agricultural watershed. Environmental Pollution, **229**, 586, **2017**.
30. CHRISTIAN B., GEORG C., LAM T.N., TRAN D.V., FRANK R. Compound-specific $\delta^{13}C$ isotopes and Bayesian inference for erosion estimates under different land use in Vietnam. Geoderma Regional, **7** (3), 311, **2016**.